Journal of Multidisciplinary Engineering Science and Technology (JMEST)
ISSN: 2458-9403
Vol. 4 Issue 2, February - 2017

Coherent Spin-valley polarization characteristics of silicene field effect transistor

Ibrahim S. Ahmed, Mina D. Asham
Dept. of Basic Engineering Science
Faculty of Engineering, Benha University
Benha, Egypt
ibrahim_maged83@yahoo.com,
minadanial@yahoo.com

Adel H. Phillips
Dept. of Engineering Physics and Mathematics
Faculty of Engineering, Ain-Shams University
Cairo, Egypt
adel.phillips@gmail.com

***Abstract*—The quantum spin and valley transport characteristics in normal silicene/ferromagnetic silicene/ normal silicene junction are investigated under the effects of magnetic field and the frequency of the induced ac-field. The spin and valley resolved conductances are deduced by solving the Dirac equation. Numerical calculations are performed and results show an oscillatory behavior to both spin and valley resolved conductances which due to resonant tunneling regime of the confined states of ferromagnetic silicene. Spin and valley polarizations are calculated. Their values show that spin and valley polarizations might be tuned by the applied gate voltage, or in other words, by electric field. The present paper is very promising for spintronics application of silicene.**

Keywords—component; Normal/ferromagnetic/ normal silicene junction; ac-field; magnetic field; spin-resolved conductance; valley-resolved conductance; spin polarization; valley polarization.

I. INTRODUCTION

In recent years new classes of materials called two-dimensional materials are synthesized [1-3]. The first identified material in this new category was graphene [3], which is a single atomic layer of carbon with a honeycomb structure. Since its discovery, in 2004, several studies have revealed the extraordinary properties of graphene, making it one of the most promising materials for applications in electronics [4], optics [5], sensors [6], and energy storage [7]. Besides the graphene, a large variety of these layered materials have been studied such as boron nitride [8,9], dichalcogenides [10-12], germanene [13-15], silicene [16-19], stanene [20], phosphorene [21,22]. Of this growing family of 2D materials, silicene has emerged to replace, not only graphene, but also bulk silicon in the current electronics, because studies have shown that silicene has electronic properties similar to those of graphene [15, 16].

Spintronics aims to exploit spin degrees of freedom instead of or in addition to charge degrees of freedom for information storage and logic devices. Compared with conventional semiconductor devices, spintronic devices have the potential advantages of nonvolatility, increased data processing speed, decreased electric power consumption, and increased integration densities [23,24].

Silicene is a monolayer of silicon atoms arranged in a honeycomb lattice structure as similar as graphene. While, as in graphene, its low-energy dynamics near the two valleys at the corner of the hexagonal Brillouin zone is described by the Dirac theory, its Dirac electrons, due to a large spin-orbit (SO) interaction, are massive with a energy gap as 1.55meV [17, 25]. Furthermore, due to the large ionic radius, silicene is buckled[10] such that the A and B sublattices of honeycomb lattice shifted vertically with respect to each other and sit in two parallel planes with a separation of 0.46nm[25, 26]. The buckled structure of silicene allows tuning its band gap via an electric field applied perpendicular to its layer. These features give many attractive properties to silicene [27-30].

To enhance the capability of conventional electronics devices based on charge degree of freedom, spintronic devices based on spin degree of freedom have become more important [31]. More recently, valley degree of freedom based on two inquivalent Dirac points at *K* and *K´*has also attracted interests [32] as a pathway towards quantum computing. The presence of large spin-orbit interaction and buckled atomic structure lead silicene to be a candidate for these growing fields of spintronics [33] and valleytronics [34]. Silicene also has stronger spin-orbit coupling which gives rise to the spin-valley coupling [35]. There have been various theoretical studies in spin valley transport at silicene junction, which helps the advancement in this area. The topics of those investigations are, for example, the electric field condition for the fully valley and spin polarized transports [36], the mechanism of magnetism opening different spin dependent band gaps at K and K´ points which results in spin and valley polarized transports [35].

The purpose of the present paper is to investigate the spin and valley polarization characteristics of normal / ferromagnetic/ normal silicene nanodevice.

II. THE MODEL

In this section we shall derive both spin polarization and valley polarization equations for silicene field effect transistor (SFET). This nanodevice is modeled as follows: a ferromagnetic silicene is

sandwiched between two normal silicenes and a metallic gate above the ferromagnetic silicene as shown in the figure below.

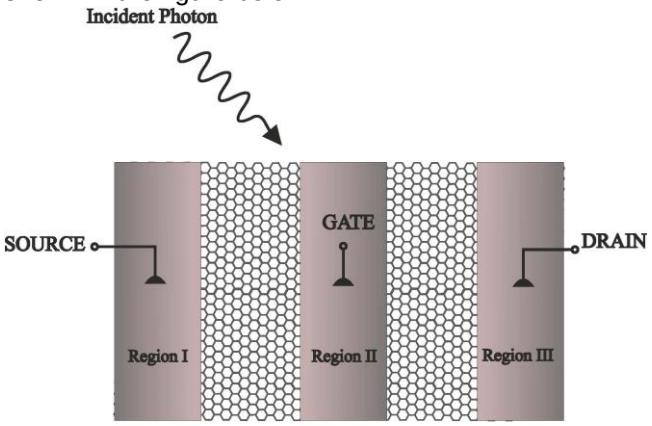

Fig. 1*Regions I & III represent normal silicene and region II represents ferromagnetic silicene.*

The transport of Dirac fermion carriers is influenced under the effect of both magnetic field and ac-field of frequency in mid infrared region. The Dirac equation is:

$$H\psi = E\psi \tag{1}$$

Where H is the Hamiltonian and it is given as [36-39]:

$$H = (\hbar v_F(\sigma_x k_x - \eta\sigma_y k_y) + \eta\sigma_z\alpha_{SOI} + U - \sigma_z h_0 + eV_{ac}\cos\omega t) \tag{2}$$

Where ħ is the reduced Planck's constant, v_F- Fermi velocity, k_x&k_y are wave vectors, $\sigma_{x,y,z}$ are Pauli matrices, α_{SOI} is the intrinsic spin orbit coupling energy in silicene , h_0 is the exchange energy of the ferromagnetic silicene, V_{ac} is the amplitude of the ac-field with frequency ω. It is noted that η=+1 for K-valley and η= -1 for K´-valley and σ=+1 for spin up and σ= -1 for spin down. The parameter U in Eq.(2) is:

$$U = V_d + eV_{sd} + eV_g + \frac{1}{2}g\mu_B B\sigma \tag{3}$$

Where V_d is the barrier height at each interface, V_{sd} is the bias voltage, V_g is the gate voltage, B – magnetic field, g –Lande g-factor and μ_B- Bohr magneton.

The eigenfunctions in regions I, II, III are obtained by solving the Dirac equation Eq.(1) which are [36-40] :

$$\psi_I = \sum_{n=1}^{\infty}\left[\frac{e^{i(k_x x+k_y y)}}{\sqrt{2E_F E_N}}\begin{pmatrix}\beta e^{i\eta\theta}\\ E_N\end{pmatrix} + \frac{r_{\eta\sigma_z}e^{i(-k_x x+k_y y)}}{\sqrt{2E_F E_N}}\begin{pmatrix}-\beta_F e^{-i\eta\theta}\\ E_N\end{pmatrix}\right]J_n\left(\frac{eV_{ac}}{n\hbar\omega}\right)e^{-in\omega t} \tag{4}$$

Also the eigenfunction in region II is:

$$\psi_{II} = \sum_{n=1}^{\infty}\left[a_{\eta\sigma_z}e^{i(k'_x x+k'_y y)}\begin{pmatrix}\beta'_F e^{i\eta\phi}\\ \varepsilon_F\end{pmatrix} + b_{\eta\sigma_z}e^{i(-k'_x x+k'_y y)}\begin{pmatrix}-\beta'_F e^{-i\eta\phi}\\ \varepsilon_F\end{pmatrix}\right]J_n\left(\frac{eV_{ac}}{n\hbar\omega}\right)e^{-in\omega t} \tag{5}$$

And the eigenfunction in region III is:

$$\psi_{III} = \sum_{n=1}^{\infty}\left[\frac{t_{\eta\sigma_z}e^{i(k_x x+k_y y)}}{\sqrt{2E_F E_N}}\begin{pmatrix}\beta_F e^{i\eta\theta}\\ E_N\end{pmatrix}\right]J_n\left(\frac{eV_{ac}}{n\hbar\omega}\right)e^{-in\omega t} \tag{6}$$

In Eqs.(4,5,6) "$J_n\left(\frac{eV_{ac}}{n\hbar\omega}\right)$" is the n^{th}-order Bessel function of first kind [41,42]. The solution of Eq.(4,5,6) must be generated by the presence of different subbands'n' in a quantum silicence nanodevice, which come with phase factor $\exp(-in\omega t)$ [41,42]. The angle θ is the incident angle on regions I & III and the angle ϕ is the incident angle on region II where they are expressed as:

$$\theta = \tan^{-1}\left(\frac{k_y}{k_x}\right) \quad and \quad \phi = \tan^{-1}\left(\frac{k'_y}{k'_x}\right) \tag{7}$$

The parametersβ_F, E_N, ε_F, k_y, k'_y, k_F and k'_F are given by:

$$\begin{aligned}\beta_F &= \hbar v_F k_F\\ E_N &= E_F + \eta\sigma_z\alpha_{SOI}\\ \varepsilon_F &= E_F - U + \sigma_z h_0 + \eta\sigma_z\alpha_{SOI}\end{aligned} \tag{8}$$

$k_y = k_F \sin\theta$ and $k'_y = k'_F \sin\phi$ (9)

$$k_F = \frac{\sqrt{E_F^2 - \alpha_{SOI}^2}}{\hbar v_F} \tag{10}$$

$$k'_F = \frac{\sqrt{\left[\left(E_F - U + \sigma_z h_0\right)^2 - \alpha_{SOI}^2\right]}}{\hbar v_F} \tag{11}$$

where E_F is the Fermi energy. In Eqs.(4, 6) the parameters $r_{\eta\sigma_z}$ & $t_{\eta\sigma_z}$ are the reflection and transmission amplitudes. Applying the boundary conditions at the interfaces we get the tunneling probability,Γ(E), as :

$$\Gamma(E) = \frac{\cos^2\theta\cdot\cos^2\phi}{\left[\cos^2(k'_x d)\cdot\cos^2\theta\cos^2\phi + \frac{\sin^2(k'_x d)\cdot\left(\gamma+\gamma^{-1}-2\sin\theta\sin\phi\right)^2}{4}\right]} \tag{12}$$

The ratio γ is:

$$\gamma = \frac{k_F \varepsilon_F}{k'_F E_N} \tag{13}$$

The wave vector k'_x is:

$$k'_x = \sqrt{\left(k'_F{}^2 - k_F^2 \sin^2\theta\right)} \tag{14}$$

The tunneling probability with the induction of ac-field $\Gamma_{ac-field}(E)$ is given by[41,42]:

$$\Gamma_{ac-field}(E) = \sum_{n=1}^{\infty} J_n^2\left(\frac{eV_{ac}}{n\hbar\omega}\right)\cdot\Gamma(E) \tag{15}$$

According to the Landauer- Buttiker equation, the conductance, G, is expressed as [40, 43]:

$$G = \frac{e^2 k_F W}{\pi^2\hbar}\cdot \int_{E_F}^{E_F+n\hbar\omega} dE \left\{\int_{-\pi/2}^{\pi/2} \Gamma_{ac-field}(E)\cdot\left(-\frac{\partial f_{FD}}{\partial E}\right)\cos\theta\cdot d\theta\right\} \tag{16}$$

where $\left(-\frac{\partial f_{FD}}{\partial E}\right)$ is the first derivative of the Fermi-Dirac distribution function and is given by:

$$\left(-\frac{\partial f_{FD}}{\partial E}\right) = \left(4k_B T\right)^{-1}\cosh^{-2}\left(\frac{E - E_F + n\hbar\omega}{2k_B T}\right) \tag{17}$$

Where k_B is the Boltzmann constant, T is the temperature, E_F is the Fermi energy, W is the width of the junction along the y-direction and d is the length of the ferromagnetic silicene.
The conductance G is computed for two cases [40,43]:

1- the valley resolved conductance is:

$$G_{K(K')} = \frac{G_{K(K')\uparrow} + G_{K(K')\downarrow}}{2} \tag{18}$$

2- the spin resolved conductance is:

$$G_{\uparrow(\downarrow)} = \frac{G_{K\uparrow(\downarrow)} + G_{K'\uparrow(\downarrow)}}{2} \tag{19}$$

The Dirac fermion conductance for both spin & valley cases are given by respectively:

$$G_{D_1} = G_\uparrow + G_\downarrow \tag{20}$$

And

$$G_{D_2} = G_K + G_{K'} \tag{21}$$

The spin polarization [40,43] is:

$$SP = \frac{\left(G_{K\uparrow} + G_{K'\uparrow}\right) - \left(G_{K\downarrow} + G_{K'\downarrow}\right)}{G_{D_1}} \tag{22}$$

And the valley polarization [40,43] is:

$$VP = \frac{\left(G_{K\uparrow} + G_{K\downarrow}\right) - \left(G_{K'\uparrow} + G_{K'\downarrow}\right)}{G_{D_2}} \tag{23}$$

III. Results and Discussion

Numerical calculations are performed for the transport characteristics parameters which are: the valley resolved conductance (Eq.18), the spin resolved conductance (Eq.19), The Dirac fermion conductance for both spin & valley cases (Eqs. 20,21), and the spin & valley polarizations (Eqs. 22,23). The values of the following parameters are [37-41,44]: v_F= 5.5x10^5 m/s, α_{SOI}= 3.9 meV, E_F= 40meV, V_d= 60meV, V_{ac}=0.25 V, Landé g-factor g=4, h_0=0.2 eV (the exchange energy of the ferromagnetic silicene), d=80 nm (length of the ferromagnetic silicene region or the channel) and W=20 nm (width of the model).
The features of the present results are:

- Figs. (2a,b,c, d) show the conductance, G, (Eq.16) versus the gate voltage, V_g,in case of both parallel and anti-parallel spin alignments and for K and K´ points at different values of the magnetic field. As shown from these figures that an oscillatory behavior of the conductance with different peak heights are observed.

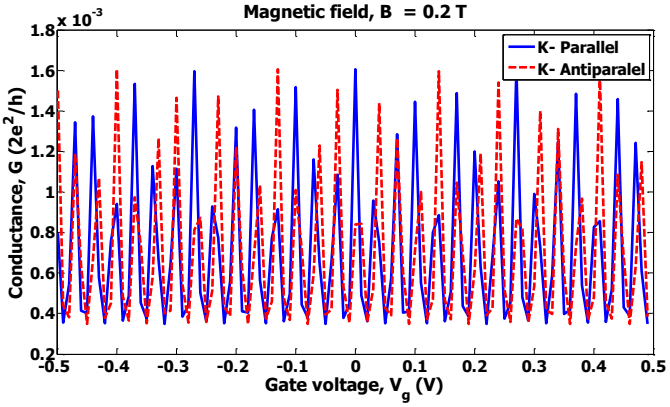

(a)

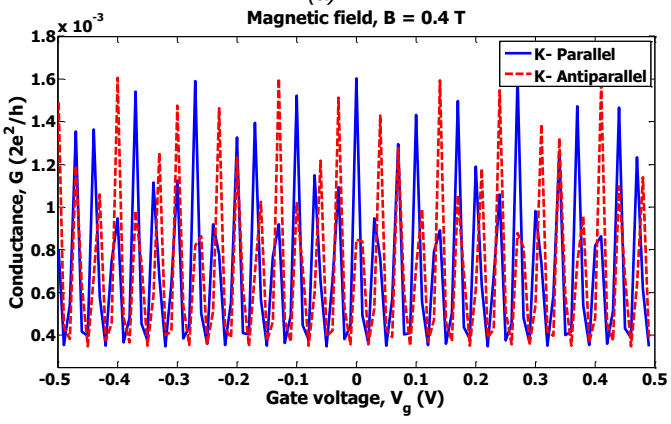

(b)

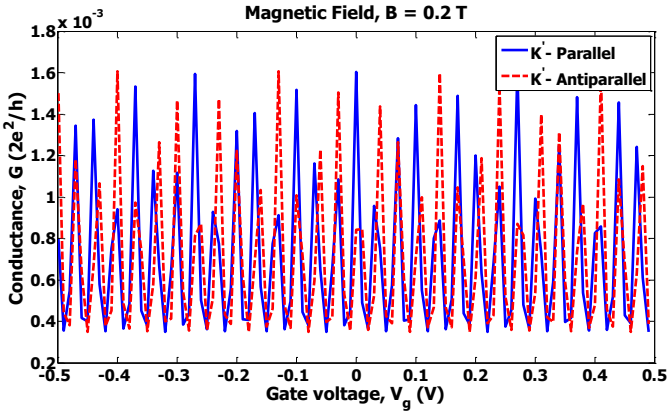

(c)

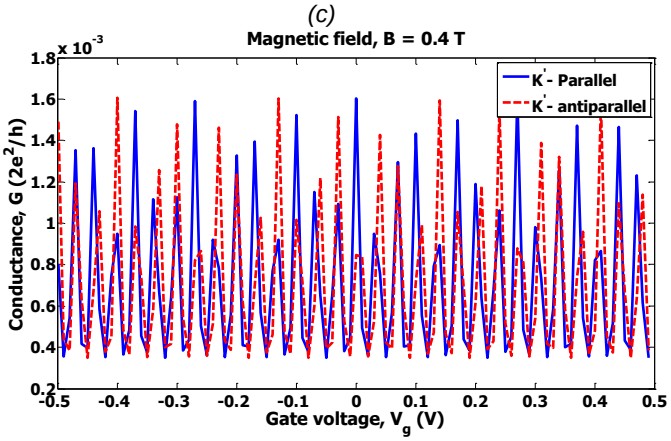

(d)

Fig. 2*The variation of the conductance, G, with the gate voltage, V_g, for parallel and antiparallel spin alignments (for K and K´ points).*

- Figs. (3a, b) show the variation of the spin resolved conductance (Eq.19) with the gate voltage in case of parallel and anti-parallel spin alignments at two different values of the magnetic field, respectively. We notice from these figures that there is very small effect due to the magnetic field on the values of the spin resolved conductance. The indication of these observations for the present silicene junction is its stability under the influence of magnetic field, which qualifies it for processing of quantum information and data storage [42, 44].

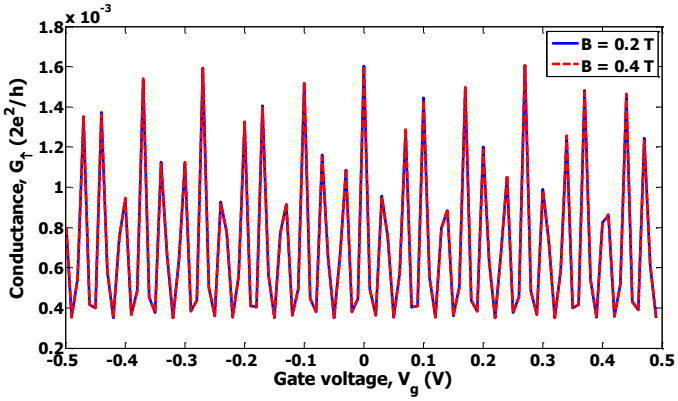

(a)

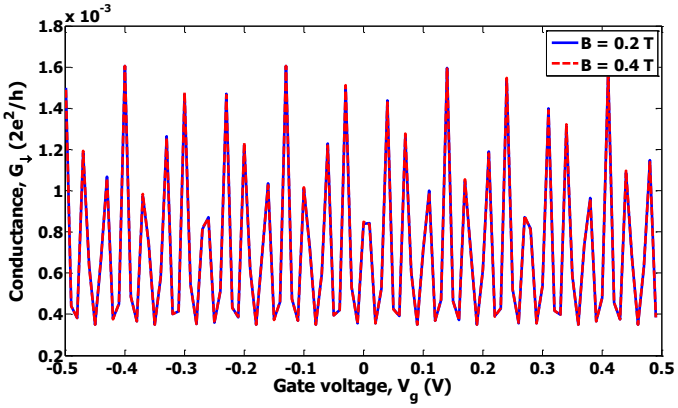

(b)

Fig. 3*The spin resolved conductance, G, vs. the gate voltage V_g for both spin up and spin down at different values of magnetic field.*

- Figs.(4a,b) show the change of the valley-resolved conductance (Eq.20) with the gate voltage Vg for K and K´ points at two different values of the magnetic field, respectively. We notice from these figures that there is no change of the valley-resolved conductance under the effect of applied magnetic field. These results show the stability of the present silicene junction which is needed for valleytronics nanodevices [35,36].

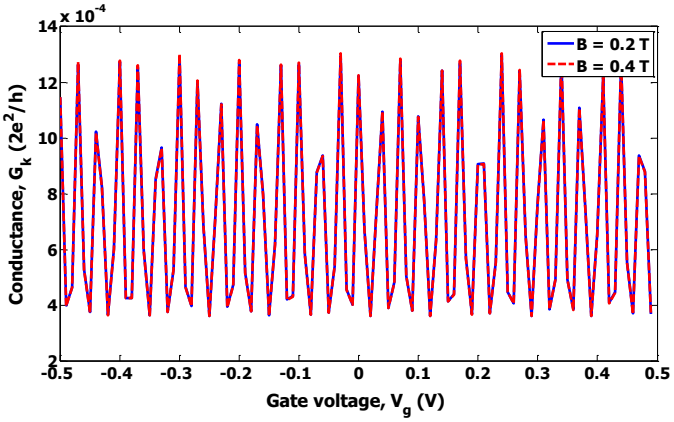

(a)

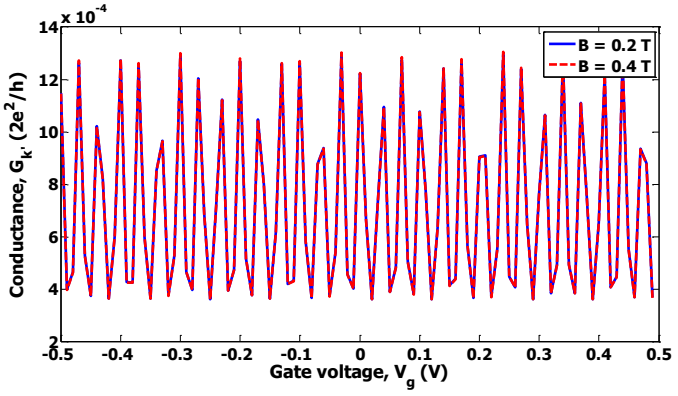

(b)

Fig. 4*The valley resolved conductance G vs. the gate voltage V_g for both K and K´ points at different magnetic fields.*

- Figs.(5a, b, c, d) show the conductance, G, (Eq.16) versus the gate voltage, V_g,in case of both parallel and anti-parallel spin alignments and for K and K´ points at different values of the frequencies (infrared range) of the induces ac-field. As shown from these figures that an oscillatory behavior of the conductance with different peak heights are observed. The present results for the conductance show that the induced far-infrared radiation introduces new photon-mediated conduction channels in the devices [41,42]. The induced ac-field enhances the energy gap, and the density of states at valleys of K and K´which exhibits photon absorption and emission. The random oscillatory behavior of the conductance results from the quantum nature of the 2D-silicene.

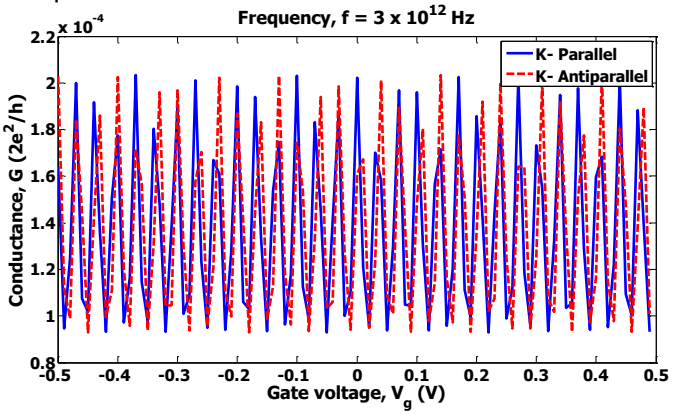

(a)

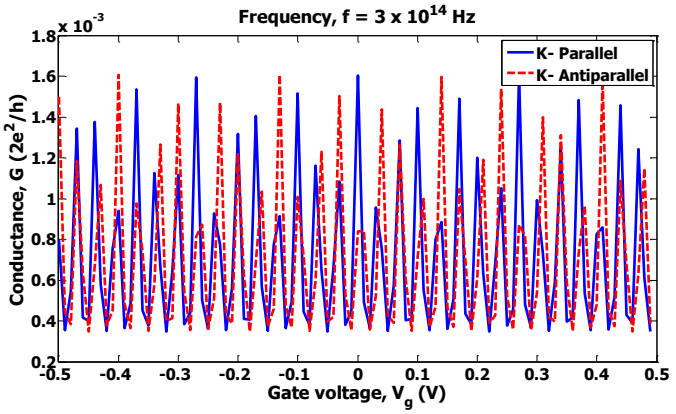

(b)

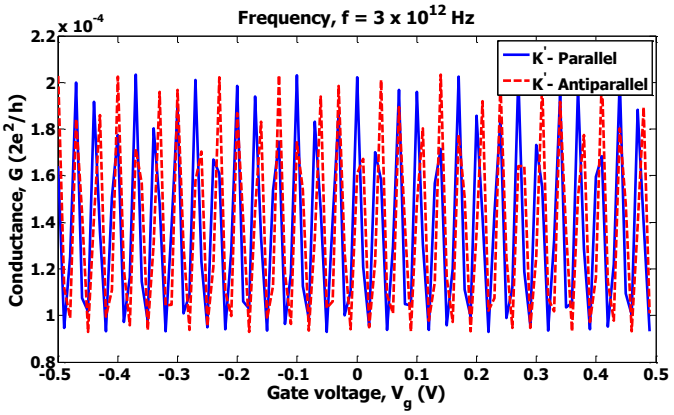

(c)

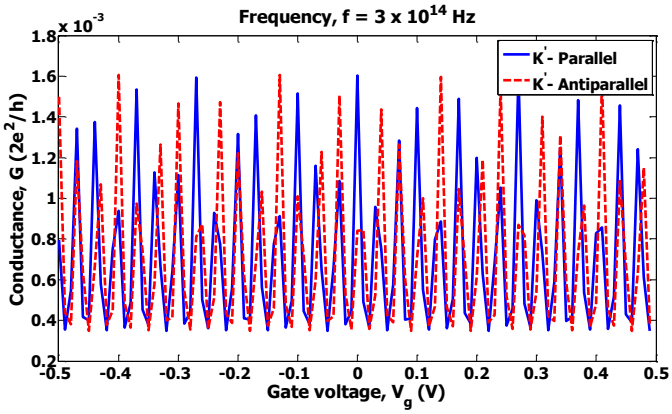

(d)

Fig. 5*The conductance, G, versus the gate voltage, V_g, for different cases of spin alignment.*

- Figs.(6a,b) show the change of the spin resolved conductance (Eq.(19)) with the gate voltage in case of parallel and anti-parallel spin alignments at different values of the frequency of ac-field.

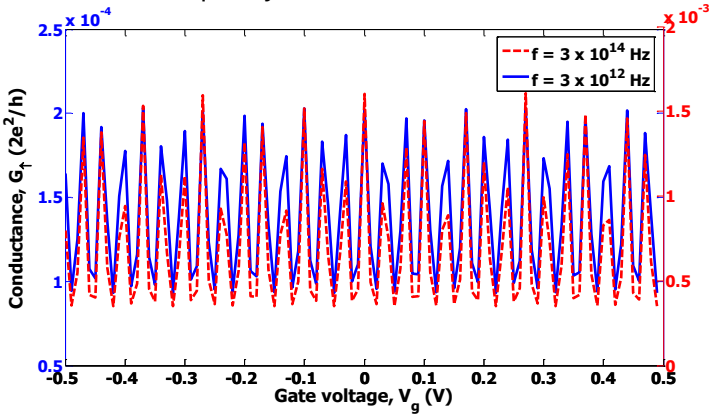

(a)

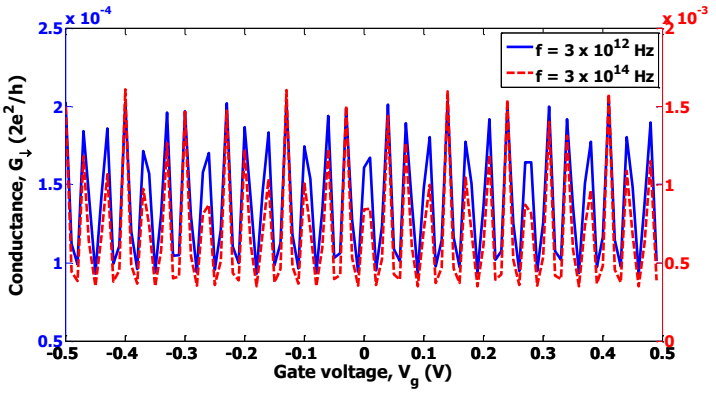

(b)

Fig. 6*The spin resolved conductance versus the gate voltage for both spin alignments.*

- Figs.(7a,b) show the variation of the valley-resolved conductance (Eq.18) with the gate voltage $V_g$for K and K´points at different values of the frequency of ac-field. As shown from Figs. (6,7) that results are due to the coupling between photons of the induced ac-field with spin and valley of the Dirac fermions electrons of silicene [41,42].

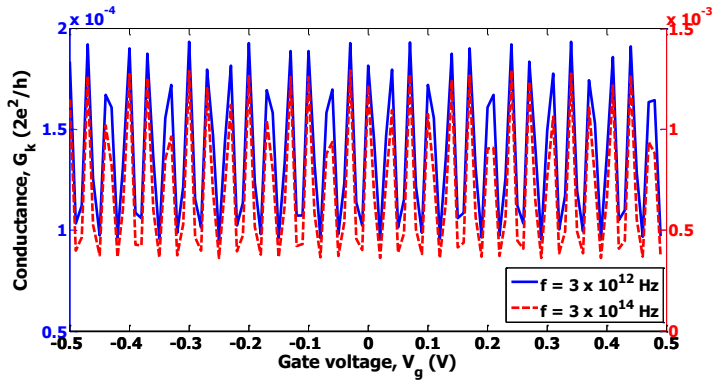

(a)

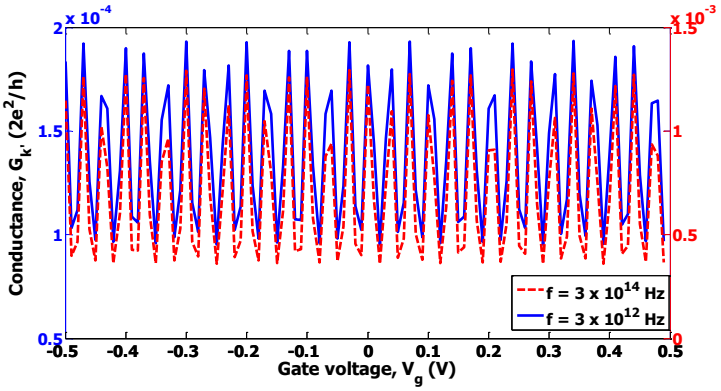

(b)

Fig. 7*The valley resolved conductance versus the gate voltage for both K and K´ points.*

- Figs.(8a,b) show the variation of spin polarization, SP, (Eq.22) with the gate voltage, V_g, at different values of the applied magnetic field and also at different frequencies of the induced ac-field respectively.

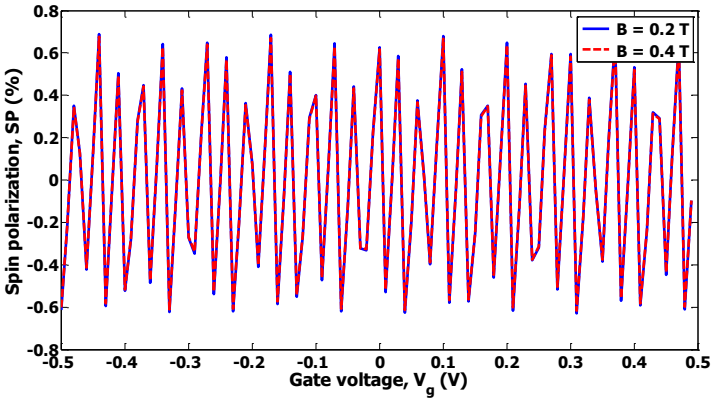

(a)

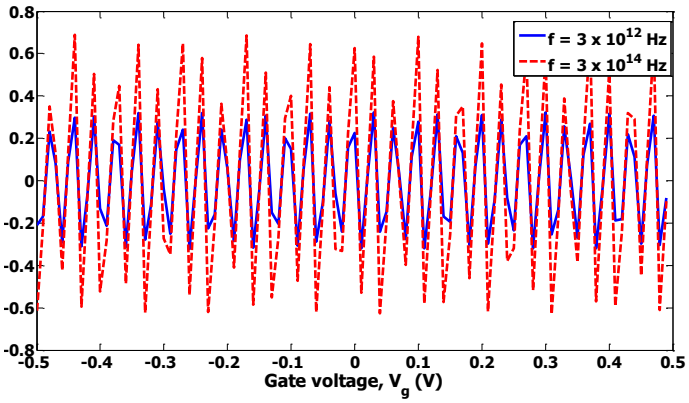

(b)

Fig. (8):*The spin polarization, SP, versus the gate voltage, Vg.*

- Figs.(9a,b) show the variation of valley polarization, VP, (Eq.23) with the gate voltage, V_g, at different values of the applied magnetic field and also at different frequencies of the induced ac-field respectively.

We notice from Figs.(8) that the spin polarization, SP, oscillates with the gate voltage, V_g, for both cases of the magnetic field and the frequency of the induced ac-field. While for valley polarization, VP, (Figs.(9)) oscillates alternatively between peaks and dips with the gate voltage under the same conditions. These results show that the current through the present investigated junction is valley and spin polarized due to the coupling between valley and spin degrees of freedom, and valley and spin polarization are tunable by local application of a gate voltage [35-40].

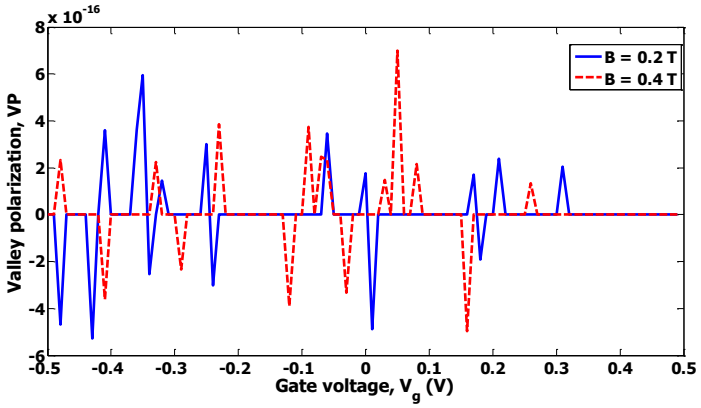

(a)

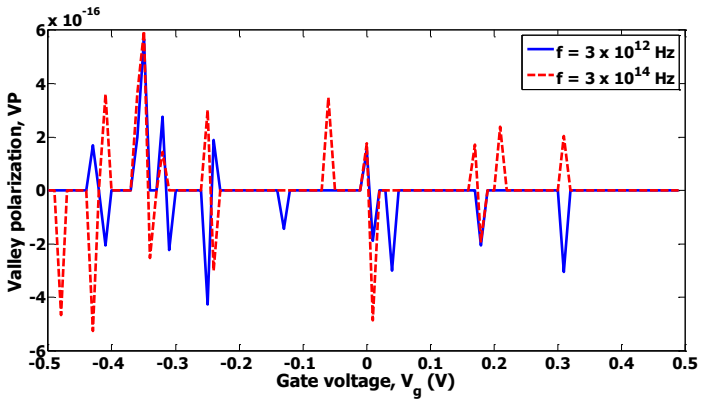

(b)

Fig.(9):*The valley polarization, VP, versus the gate voltage, Vg.*

In general results show that the conductance, spin and valley resolved conductance in the present junction oscillate with the gate voltage under the effects of both frequency of the induced ac-field and the applied magnetic field. This might be considered that the present investigated junction as resonant tunneling nanodevice. Also results show that the Dirac fermion carrier transport through this junction is spin and valley polarized due to the coupling between valley and spin degrees of freedom, and the valley and spin polarizations can be tuned by local application of a gate voltage.

IV. Conclusion

The present paper studied theoretically the spin-valley transport through normal silicene/ ferromagnetic silicene/ normal silicene junction. The spin-resolved conductance and valley-resolved conductance are deduced by solving Dirac equation under the effects of the frequency of ac-field and the applied magnetic field. Results show oscillatory behavior of the considered conductance. Computation of spin and valley polarizations provides the scientific interests that how to construct spin-valley filter for silicene based logic applications of nanoelectronics devices. We might expect that the present junction could be realized experimentally for spin-valleytronics nanodevices.

References

[1] K. S. Novoselov, A. K. Geim, S. V. Morozov, D. Jiang, Y. Zhang, S. V. Dubonos, I. V. Grigorieva, and A. A. Firsov,"Room-temperature electric field effect and carrier-type inversion in graphene films,"Science306, 666 (2004).

[2] A. K. Geim, "Graphene: Status and Prospects,"Science324, 1530 (2009).

[3] P. Miro, M. Audiffred and T. Heine, "An atlas of two-dimensional materials," Chem. Soc. Rev., 43, pp.6537-6554(2014).

[4] M. Woszczyna, A. Winter, M. Grothe, A. Willunat, S. Wundrack, R. Stosch, T. Weimann, F. Ahlers and A. Turchanin, "All-carbon vertical van der Waals heterostructures:Non-destructive functionalization of graphene for electronic applications,"Adv. Mater., 26, pp.4831-4837 (2014).

[5] G. Jo, M. Choe, S. Lee, W. Park, Y. H. Kahn and T. Lee, "The application of graphene as electrodes in electrical and optical devices," Nanotechnology, 23, 112001(2012).

[6] Y. Wang, L. Wang, T. Yang, X. Li, X. Zang, M. Zhu, K. Wang, D. Wu and H. Zhu, "Wearable and Highly Sensitive Graphene Strain Sensors for Human Motion Monitoring," Adv. Funct. Mater., 24, pp.4666-4670 (2014).

[7] J. Zhu, D. Yang, Z. Yin, Q. Yan and H. Zhang, "Graphene and Graphene-Based Materials for Energy Storage Applications," Small, 2014, 10, pp.3480-3498.

[8] L. Song, L. Ci, H. Lu, P. B. Sorokin, C. Jin, J. Ni, A. G. Kvashnin, D. G. Kvashnin, J. Lou, B. I. Yakobson and P. M. Ajayan, "Large Scale Growth and Characterization of Atomic Hexagonal Boron Nitride Layers," Nano Lett., , 10, pp.3209-3215(2010).

[9] H. Sahin, S. Cahangirov, M. Topsakal, E. Bekaroglu, E. Akturk, R. T. Senger and S. Ciraci, "Monolayer honeycomb structures of group IV elements and III-V binary compounds," Phys. Rev. B, 80, 155453(2009).

[10] M. Chhowalla, H. S. Shin, G. Eda, L.-J. Li, K. P. Loh and H. Zhang, "The chemistry of two-dimensional layered transition metal dichalcogenide nanosheets," Nat. Chem, 5, pp.263-275 (2013).

[11] Q. H. Wang, K. Kalantar-Zadeh, A. Kis, J. N. Coleman and M. S. Strano, "Electronics and optoelectronics of two-dimensional transition metal dichalcogenides," Nat. Nano, 7,pp. 699-712(2012).

[12] S. Z. Butler, S. M. Hollen, L. Cao, Y. Cui, J. A. Gupta, H. R. Gutiérrez, T. F. Heinz, S. S. Hong, J. Huang, A. F. Ismach, E. Johnston-Halperin, M. Kuno, V. V. Plashnitsa, R. D. Robinson, R. S. Ruoff, S. Salahuddin, J. Shan, L. Shi, M. G. Spencer, M. Terrones, W. Windl and J. E. Goldberger, "Progress, Challenges, and Opportunities in Two-Dimensional Materials Beyond Graphene," ACS Nano, 7, pp.2898-2926(2013).

[13] J. C. Garcia, D. B. de Lima, L. V. C. Assali and J. F. Justo, "Group-IV graphene- and graphane-like nanosheets," J. Phys. Chem. C., 115, pp.13242-13246(2011).

[14] S. Balendhran, S. Walia, H. Nili, S. Sriram and M. Bhaskaran, "Elemental Analogues of Graphene: Silicene, Germanene,Stanene, and Phosphorene," Small, 11, pp.640-652 (2015).

[15] S. Cahangirov, M. Topsakal, E. Akturk, H. Şahin and S. Ciraci, "Two- and one-dimensional honeycomb structures of silicon and germanium," Phys. Rev. Lett., 102, 236804 (2009).

[16] S. Lebègue and O. Eriksson, "Electronic structure of two-dimensional crystals from ab-initioTheory," Phys. Rev. B, 79, 115409(2009).

[17] C.-C. Liu, W. Feng and Y. Yao, "Quantum Spin Hall Effect in Silicene," Phys. Rev. Lett., 2011, 107, 076802.

[18] X. Lin and J. Ni, "Much stronger binding of metal adatoms to silicene than to graphene: A first-principles study," Phys. Rev. B, 86, 075440(2012).

[19] D. Jose and A. Datta, "Structures and Chemical Properties of Silicene:Unlike Graphene," Acc. Chem. Res., 2014, 47, pp.593-602.

[20] Y. Xu, B. Yan, H.-J. Zhang, J. Wang, G. Xu, P. Tang, W. Duan and S.-C. Zhang, "Large-gap quantum spin Hall insulators in tin films," Phys. Rev. Lett., 111, 136804(2013).

[21] H. Liu, A. T. Neal, Z. Zhu, Z. Luo, X. Xu, D. Tomanek and P. D. Ye, "Phosphorene: An Unexplored 2D Semiconductor with a High Hole Mobility," ACS Nano, 8, 4033-4041(2014).

[22] F. Xia, H. Wang and Y. Jia, "Rediscovering black phosphorus as an anisotropiclayered material for optoelectronics and electronics," Nat. Commun, 5, 5458(2014).

[23] Jongyeon Kim, Ayan Paul, Paul A. Crowell, Steven J. Koester, Sachin S. Sapatnekar, Jian-Ping Wang, and Chris H. Kim, "Spin-Based Computing: Device Concepts, Current Status, and a Case Study on a High-Performance Microprocessor," Proceedings of the IEEE, Vol. 103, No. 1, pp.106-130, (2015).

[24] Ahmed S. Abdelrazek, Walid A. Zein and Adel H. Phillips, "Spin-dependent Goos-Hanchen effect in semiconducting quantum dots," SPIN (World Scientific) vol.3, No.2, 1350007 (2013).

[25] N. D. Drummond, V. Zólyomi, and V. I. Fal'ko, "Electrically tunable band gap in silicene," Phys. Rev. B 85, pp.075423-075429 (2012).

[26] Z. Ni, Q. Liu, K. Tang, J. Zheng, J. Zhou, R. Qin, Z. Gao, D. Yu, and J. Lu, "Tunable Bandgap in Silicene and Germanene," Nano Lett. 12, pp.113 (2012).

[27] M. Ezawa, "Photo-Induced Topological Phase Transition and a Single Dirac-Cone Statein Silicene," Phys. Rev. Lett. 110, pp.026603-026607 (2013).

[28] W.-F. Tsai, C.-Y. Huang, T.-R. Chang, H. Lin, H.-T. Jeng, and A. Bansil, "Gated Silicene as a tunable source of nearly 100% spin-polarized," Nature Communications 4, pp.1500 (2013).

[29] C. J. Tabert, and E. J. Nicol, "Valley-Spin Polarization in the Magneto-Optical Response of Silicene and Other Similar 2D Crystals," Phys. Rev. Lett. 110, (2013) 197402.

[30] H. Pan, Z. Li, C.-C. Liu, G. Zhu, Z. Qiao, and Y. Yao, "Valley-Polarized Quantum Anomalous-Hall Effects in Silicene," Phys. Rev. Lett. 112, pp.106802 (2014).

[31] S. A. Wolf, D. D. Awschalom, R. A. Buhrman, J. M. Daughton, S. von Molnar, M. L. Roukes, A. Y. Chtchelkanova, D. M. Treger, "Spintronics: A Spin-Based Electronics Vision for the Future," Science 294, 1488 - 95(2001).

[32] E. J. Sie, J. W. McIver, Y. H. Lee, L. Fu1, J. Kong and N. Gedik, "Valley-selective optical Stark effect in monolayer WS_2," Nature Materials 14, pp.290–294 (2015).

[33] Y. Wang, R. Quhe, D. Yu, J. Li, J. Lu, "Silicene Spintronics-A Concise Review," Chinese Physics B, 24, No.8, 087201 (2015).

[34] M. Ezawa, "Spin-Valleytronics in Silicene: Quantum-Spin-Quantum-Anomalous Hall Insulators and Single-Valley Semimetals," Physical Review B 87, 155415 (2013).

[35] T. Yokoyama, "Spin and valley transports in junctions of Dirac fermions," New Journal Physics 16, 085005 (2014).

[36] T. Yokoyama, "Controllable valley and spin transports in ferromagnetic silicene junctions," Physical Review B 87, 241409 (2013).

[37] C. C. Liu, H. Jiang and Y. G. Yao, "Low-energy effective Hamiltonian involving spin-orbit coupling in Silicene and Two Dimensional Germanium and Tin," Phys. Rev. B84, 195430 (2011).

[38] Y. Wang, and Y. Lou, "Giant tunneling magnetoresistance in silicene," J. Appl. Phys. 114, 183712 (2013).

[39] M. M. Grujic, M. Z. Tadic and F. M. Peeters, "Spin-Valley Filtering in Strained Graphene Structures with Artificially Induced Carrier Mass and Spin-Orbit Coupling," Phys. Rev. Lett. , 113, 046601 (2014).

[40] X. Q. Wu and H. Meng, "Gate-tunable valley-spin filtering in silicene with magnetic barrier," J. Appl. Phys., 117, 203903 (2015).

[41] G. Platero, and R. Aguado, "Photon assisted transport in semiconductor nanostructures," Phys Rep, 395, 1 (2004). https://doi.org/10.1016/j.physrep.2004.01.004.

[42] Ahmed Saeed Abdelrazek, Mohamed Mahmoud El-banna, and Adel Helmy Phillips, "Photon-spin coherent manipulation of piezotronic nanodevice," Micro & Nano Letters, , 11, Iss. 12, pp. 876–880 (2016) doi: 10.1049/mnl.2016.0264.

[43] B. Soodchomshom, "Perfect spin-valley filter controlled by electric field in ferromagnetic silicene," J. Appl. Phys., 115. 023706 (2014).

[44] M. D. Asham, W. A. Zein and A. H. Phillips, "Photo-induced spin dynamics in nanoelectronic devices," Chin. Phys. Lett. 29 (10), 108502 (2012).